Bootstrap-based Confidence Interval Estimation for Thermal Security Region of China Southern Power Grid

Xue Li[1], *Tao Jiang*[1*], *Guodong Liu*[2 *], Hantao *Cui*[3], *and Fangxing Li*[3]

[1]: *Department of Electrical Engineering, Northeast Electric Power University, Jilin, JL 132012, China*
[2]: *Power and Energy Systems Group, Oak Ridge National Laboratory, Oak Ridge, TN 37831, USA*
[3]: *Department of Electrical Engineering and Computer Science, University of Tennessee, Knoxville, TN 37996, USA*
[*]: Contact author: tjiang@neepu.edu.cn, liug@ornl.gov

Abstract— Thermal security region (TSR) is a powerful tool for monitoring and controlling the thermal security in bulk power grid with high penetration of renewable energy. One of the major challenges of TSR in application is to obtain the exact analytical expression of the TSR boundary (TSRB) due to the fact that TSRB is a nonlinear hypersurface described by an implicit function. For this reason, the TSRB is usually approximated using hyperplane instead of getting the exact analytical expression. Traditionally, the coefficients of the hyperplane are estimated with set of original TSRB points using least square estimation (LSE). However, LSE is a point estimation method, which is incapable of evaluating the quality of the estimation. In addition, the accuracy and computational efficiency of the hyperplane approximation are influenced by the number of TSRB points significantly. In this paper, a bootstrap based confidence interval estimation is proposed to estimate not only the coefficients of TSRB approximation hyperplane, but also the standard deviations and confidence intervals of the coefficients for evaluating the quality and reliability of the approximation results. First, empirical distribution functions (EDFs) of the coefficients of TSRB approximation hyperplane are approximated from set of original TSRB points by using residual resampling bootstrap method. Then, the EDFs of the coefficients are employed to estimate the coefficients of the approximation hyperplane. Meanwhile, the standard deviations and confidence intervals of the estimated coefficients of the hyperplanes are also calculated for evaluating the quality and reliability of the approximation. The proposed approach is tested on the China Southern Power Grid (CSG). Results of simulations validate the accuracy and efficiency of the proposed approach in approximating the TSRB.

Keywords—bootstrap, confidence interval, thermal security region, hyperplane

1. Introduction

With growing penetration of intermittent renewable energy sources and increasing variability of generation dispatch, the patterns of power flow have become more diverse and further deviating from the pre-designed conditions, leading to more uncertainty and risks for bulk power grid operation [1]. To mitigate the impacts of intermittent renewable resources on the power grid, new wide-area balancing coordination and cooperation schemes have been implemented [2]. These schemes enable the power flow redistribution in the wide area. Nevertheless, the growing variability still presents a challenge for maintaining the thermal security for a bulk power system with *N*-1 contingency. For this reason, the widely used single-directional limited analysis methods, which only consider the thermal security constraints in a specified power grid stress direction, are ineffective because they are unable to account for the coupling interactions between the transmission interties at the system-wide level [3]. Moreover, the intermittency of renewable energy sources and the variability of generation dispatch might change the stress direction which cause the results of the single-directional limited analysis method seriously departure from the actual operation condition [4]. Under this situation, the transmission thermal constraints should be revisited in terms of their definition, structure and characteristics [3], [4]. This necessity is addressed by thermal security region (TSR).

The TSR is defined as a *n*-dimensional set of nodal power injections or total power on the transmission corridor, in which the power flow equations and the thermal security constraints are satisfied[5], [6]. Generally, the TSR composed of *n* dimensional

manifolds is a continuous region, in which the power grid is thermal security in case of N-1 contingency, while TSR boundary (TSRB) composed of n-1 dimensional manifolds is a nonlinear hypersurface on which the power grid is at the status of critical thermal security with N-1 contingency [3]. Using the TSR, the bulk power gird thermal security evaluation could be fast and convenient by simply determining whether the operation point is inside or outside the TSR. The key to this type of thermal security evaluation is to determine the TSRB, which separates the secure power grid conditions from the insecure ones and is described by an implicit function. However, the exact analytical expression of TSRB is very difficult to obtain due to the nonlinearity of TSRB. To address this issue, artificial neural network (ANN) was used to approximate the security region boundary considering the nonlinearity [7], [8]. However, the ANN requires huge volumes of training samples to formulate the approximation model of security region boundary. Meanwhile, the physical information of power grid is hidden in the black box, which makes it hard to provide more underlying information for making control decisions. The sampling-fitting method, which is a major type of TSRB approximation was proposed in [9], [10]. In this method, the critical operation points on the TSRB are explored by repeated power flow (RPF) or optimal power flow (OPF) with different power gird stresses. Then, these explored TSRB points are fit to certain analytical expressions to approximate the TSRB. In [11], Prof. Y. Yu *et al*. found that the security region boundary could be well represented by a hyperplane. The pointwise sampling and least square estimation (LSE) were proposed to estimate the coefficients of the hyperplane [12],[13]. The analytical expression of hyperplane was easily estimated. If one hyperplane does not meet the desired accuracy level of approximation, more hyperplanes can be employed to improve the approximation accuracy. Using the estimated TSRB hyperplanes, the thermal security margin can be directly calculated, and the corrective control actions can be determined conveniently. Similar ideas were also used in the Western Electricity Coordinating Council (WECC) system and the European Network of Transmission System Operators for Electricity (ENTSO-E) [3], [14]. However, due to fact that the sampling-fitting method is a typical point estimation method, there are still some issues, such as lacking guarantee on the quality and reliability of the estimated results. The confidence interval (CI) estimation may offer solutions to these issues.

Traditionally, the CIs of given statistical parameters can be estimated using Monte Carlo method through numerical simulation. The Monte Carlo method can calculate the means and standard deviations of the statistical parameters by repeated random sampling. However, the Monte Carlo method is a model dependent method, the numerical simulation should sample from an already known probability distribution of each variable in the power grid, which is infeasible in practice. Moreover, to achieve accurate and reliable estimation of the hyperplane coefficients, the Monte Carlo method needs large amounts of TSRB points explored with numerous stress directions, which significantly increases the computational burden. Under such situations, it is very difficult to use Monte Carlo method to estimate the CIs for the coefficients of TSRB approximation hyperplane in a limited time frame. Bootstrap method can address this problem.

The Bootstrap method originally introduced in [15] is a general resampling technique for estimating the distributions and CIs of statistics from identical independent observations. Comparing with the Monte Carlo method, the bootstrap method has the following advantages: ①the bootstrap method uses the original samples as the population to resample, whereas the Monte Carlo simulation resamples by setting up a random sample generation process with known values of the parameters; ②The distribution of parameters is unnecessary for the bootstrap method, but it is essential for Monte Carlo method; ③The bootstrap method is a model-free method, while the Monte Carlo method is a model-dependent method. Using the Monte Carlo method to estimate the CIs of statistics requires the already known model. Due to the aforementioned advantages, the bootstrap method has been widely used in the power systems for available transfer capability (ATC) assessment [16] , electromechanical oscillation mode estimation [17], power system optimal scheduling[18], long-term operation planning[20], electricity price forecasting [20], electricity demand forecasting [21], wind power forecasting [22], distribution system reliability evaluation [23], and transmission reliability margin determination [24]. In this paper, the bootstrap method is introduced to provide the CI estimation of the coefficients of the TSRB approximation hyperplanes for the first time. An initial regression model for the TSRB approximation hyperplane is estimated using the original TSRB points tracked by RPF. Then, residual resampling is used to bootstrap the synthetic response variables based on the predicted values and the residuals which are calculated through the estimated initial regression model. Regressing these bootstrapped synthetic response variables on the fixed independent variables drawn from the original TSRB points, the coefficients of TSRB approximation hyperplane are solved. Repeat above procedure with large number of times by using resampling with replacement, the empirical distribution functions (EDFs) of the hyperplane coefficients are extracted, and then the bootstrap means, standard deviations and CIs of the coefficients for TSRB approximation hyperplane are estimated from the constructed EDFs of the coefficients. The major contributions of this work are as follows.

1) The CI estimation is introduced to estimate the TSRB approximation hyperplane, and further measure the quality and reliability of the estimated results.
2) A bootstrap regression model for the TSRB approximation hyperplane is developed and solved by residual resampling to obtain the means, standard deviations and CIs of the coefficients of the TSRB approximation hyperplanes.

The rest of this paper is organized as follows. Section 2 reviews the characteristics of TSRB with *N*-1 contingency. Section 3 proposes a hyperplane-based approximation approach to approximate the TSRB to build the TSR. Section 4 develops a bootstrap based CI estimation approach to solve the approximation hyperplane. Section 5 validates the performance of the developed methods by using the numerical simulations in China Southern Grid (CSG). Finally, Section 6 draws the conclusions.

2. TSR with *N*-1 Contingency

In power grid, the set of the thermal constraints of the branches can be expressed as [25], [26]:

$$\Re_T := \left\{ i_k \in \boldsymbol{R} \middle| -i_k^{\max} \le i_k \le i_k^{\max}, \forall k \in \boldsymbol{B} \right\} \tag{1}$$

where，$\Re_T$ is a set of the thermal constraints for all the branches in the power grid; $\boldsymbol{B}$ is a set of branches; i_k is the current on the kth branch. The superscript max means the upper limit of the current on the branch.

According to the thermal constraints of the branches expressed in (1), the TSR of power grid can be defined as a set of operation points which satisfy the power flow equation constraint and thermal constraint. Hence, the TSR can be represented as

$$\Omega_T := \left\{ \boldsymbol{D} \subset \boldsymbol{R}^n \middle| i_k \in \Re_T, f\left(\boldsymbol{x}, \boldsymbol{y}\right) = 0 \right\} \tag{2}$$

where, Ω_T is TSR of power gird; $f(\boldsymbol{x}, \boldsymbol{y})$ is power flow equation；$\boldsymbol{x}$ is a vector of state variables in power grid；$\boldsymbol{y}$ is a vector of power injections at buses; $\boldsymbol{D}$ is a vector of descriptor variables reflecting the most influential or understandable combinations of parameters that influence the system security margin such as current on branch, power flow on the certain path, total generation, total area load, voltage of bus; n is the dimension of $\boldsymbol{D}$.

In practical power grid, the operators not only concern the thermal security problem at current operation point, but also pay attention to the thermal security post N-1 contingency at the operation point. Therefore, the TSR of power grid satisfying the N-1 contingency can be formulated as：

$$\Omega_T := \left\{ \boldsymbol{D} \subset \boldsymbol{R}^n \middle| \forall \Im, i_k \in \Re_T, f\left(\boldsymbol{x}, \boldsymbol{y}\right) = 0 \right\} \tag{3}$$

where $\Im$ is a set of N-1 contingency.

According to the definition of TSR with N-1 contingency as in (3)，it can be inferred that, for the critical operation point on the TSRB, there is at least one branch at the critical status of the thermal security.

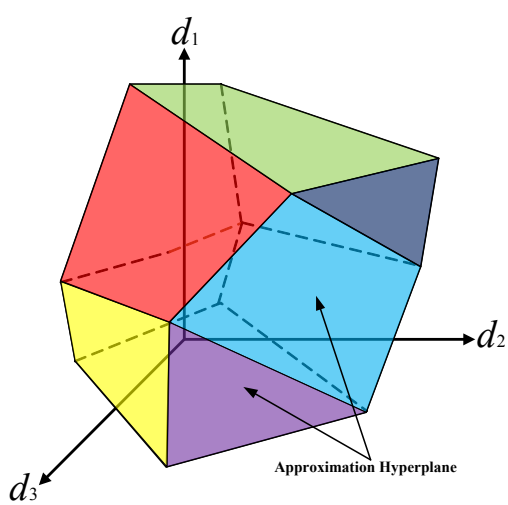

Fig.1 Thermal stability region boundary proximated by hyperplanes

3. TSRB Approximation

In the power grid, although a set of the thermal security critical points with N-1 contingency on the TSRB can be tracked by using RPF or OPF, there is rarely existing an exact analytical expression to discrible this boundry. Hence, the tracked TSR is

inefficient to guide the power grid operators in operation. To address this issue and implment the TSR on the power gird operation, the authors of [11] points out that the TSRB can be approximated by hyperplanes. Fig.1 shows the TSRB with multiply thermal secutiry constraints approximated by hyperplanes, and the hyperplanes approximating TSRB can be described as a set of equalities [26]

$$\begin{cases} \boldsymbol{\beta}_1\bar{\boldsymbol{d}}_1 = \beta_{1,0}\bar{d}_{1,1} + \beta_{1,1}\bar{d}_{1,2} + \cdots + \beta_{1,n}\bar{d}_{1,n} = i_1^{\max} \\ \boldsymbol{\beta}_2\bar{\boldsymbol{d}}_2 = \beta_{2,0}\bar{d}_{2,1} + \beta_{2,1}\bar{d}_{2,2} + \cdots + \beta_{2,n}\bar{d}_{2,n} = i_2^{\max} \\ \quad\vdots \\ \boldsymbol{\beta}_k\bar{\boldsymbol{d}}_k = \beta_{k,0}\bar{d}_{k,1} + \beta_{k,1}\bar{d}_{k,2} + \cdots + \beta_{k,n}\bar{d}_{k,n} = i_k^{\max} \\ \quad\vdots \\ \boldsymbol{\beta}_l\bar{\boldsymbol{d}}_l = \beta_{l,0}\bar{d}_{l,1} + \beta_{1,1}\bar{d}_{l,2} + \cdots + \beta_{l,n}\bar{d}_{l,n} = i_l^{\max} \end{cases} \tag{4}$$

where $\boldsymbol{\beta}_k=[\beta_{k,0}, \beta_{k,1}, \cdots, \beta_{k,n}]$ is the coefficient vector of kth hyperplane approximating the TSRB with respect to the thermal constraint of the kth branch; $\bar{\boldsymbol{d}}_k = \left[\bar{d}_{k,1} \quad \bar{d}_{k,2} \quad \cdots \quad \bar{d}_{k,n}\right]$ is a vector of descriptor variables at the thermal security critical point on the TSRB with respect to the thermal constraint of the kth branch; $i_k^{\max}$ is the upper limit of current on the kth branch； n is a dimension of TSR。

With the approximated TSRB in (4), the current operation point, $\boldsymbol{d} = \left[d_1, d_2, \cdots, d_n\right]$ can be simply assessed for the thermal security in case of any N-1 contingency. If $\boldsymbol{d} = \left[d_1, d_2, \cdots, d_n\right]$ satisfy the set of linear inequalities in (5), the power grid can be considered as thermal secure in case of any N-1 contingency [3], [4]. Otherwise, a thermal security violation might happen.

$$\begin{cases} \boldsymbol{\beta}_1\boldsymbol{d} = \beta_{1,0}d_1 + \beta_{1,1}d_2 + \cdots + \beta_{1,n}d_n \le i_1^{\max} \\ \boldsymbol{\beta}_2\boldsymbol{d} = \beta_{2,0}d_1 + \beta_{2,1}d_2 + \cdots + \beta_{2,n}d_n \le i_2^{\max} \\ \quad\vdots \\ \boldsymbol{\beta}_k\boldsymbol{d}_k = \beta_{k,0}d_1 + \beta_{k,1}d_2 + \cdots + \beta_{k,n}d_n \le i_k^{\max} \\ \quad\vdots \\ \boldsymbol{\beta}_l\boldsymbol{d} = \beta_{l,0}d_1 + \beta_{1,1}d_2 + \cdots + \beta_{l,n}d_n \le i_l^{\max} \end{cases} \tag{5}$$

It is obvious that the TSRB approximated by hyperplane in (4) is very convenient for evaluating the power grid thermal security, calculating the thermal security margin, identifying weak elements influencing the security margin and potentially providing useful information for making control decisions. However, Determining the coefficients of hyperplanes in (4) is critical for the application of TSR. Currently, the general method to solve the coefficients of hyperplanes is to explore the huge volume of TSRB points with multiply stress directions by RPF, then estimates the coefficients of hyperplanes as (6) by using LSE

$$\boldsymbol{\beta}_k^T = i_k^{\max}\left(\bar{\boldsymbol{D}}_k^{\mathrm{T}}\bar{\boldsymbol{D}}_k\right)^{-1}\bar{\boldsymbol{D}}_k^{\mathrm{T}}\boldsymbol{L} \tag{6}$$

where $\bar{\boldsymbol{D}}_k = \left[\bar{\boldsymbol{d}}_{k,1}, \bar{\boldsymbol{d}}_{k,2}, \cdots, \bar{\boldsymbol{d}}_{k,i}\right]$ is a set of TSRB points with respect to the thermal constraint of the kth branch, $\boldsymbol{L} = \left[1, 1, \cdots, 1\right]$, $\boldsymbol{L} \in \boldsymbol{R}^n$.

Using (6), all the coefficients of hyperplanes approximating the TSRB with respect to the thermal security of the concerned branches with N-1 contingency are solved, and the TSR with detailed hyperplane expression is then acheived.

Further, to evaluate the approximation accuracy of TSRB by using the hyperplane, the relative error is defined as [27]:

$$\rho_{i,k} = \frac{\left|\beta_{k,0}\bar{d}_{k,1} + \beta_{k,1}\bar{d}_{k,2} + \cdots + \beta_{k,n}\bar{d}_{k,n} - i_k^{\max}\right|}{i_k^{\max}} \times 100\% \tag{7}$$

Theoretically, the more precisely the hyperplane approximates the TSRB, the more TSRB points are required. However, more TSRB points mean more computational time in TSRB point tracking. To address this issue, a bootstrap-based CI estimation approach is developed in this work to determine the accurate coefficients of hyperplanes which approximate the TSRB precisely.

4. Bootstrap based CI Estimation for TSRB Approximation Hyperplane

As mentioned earlier, the TSRB can be approximated by hyperplanes via the LSM, and the approximation accuracy depends on the number of the TSRB points, however, tracking huge amount of TSRB points will aggravate the computational burden which is an obstacle for TSR online application. Moreover, the LSM, a typical point estimation method, is unable to evaluate the quality and the reliability of the estimated results. To deal with these issues, a bootstrap based CI estimation is developed in this section to solve the coefficients of the TSRB approximation hyperplanes.

4.1. Bootstrap method

The bootstrap method originally developed in [15] is a very general resampling technique for estimating the distributions of statistics based on independent observations by sampling an original observation dataset with replacement to create large number of datasets. It has been successfully demonstrated in mathematics, statistics, physics, engineering, behavioral and life science. The general idea of bootstrap is based on resampling from a given sample set. Given a set of independent and identically distributed (IID) observation $\boldsymbol{x}=\{x_1, x_2, \cdots, x_m\}$ and dataset $\theta(\boldsymbol{x})$ statistically estimated from $\boldsymbol{x}=\{x_1, x_2, \cdots, x_m\}$. Using the basic bootstrap method to estimate the mean μ and standard deviation σ of $\theta(\boldsymbol{x})$ can be summarized as follows:

1) Randomly draw s samples from a given observation dataset $\boldsymbol{x}=\{x_1, x_2, \cdots, x_m\}$ where $m> s$ to form a bootstrap dataset $\boldsymbol{x}_i^*=\{x_1, x_2, \cdots, x_s\}$.
2) Repeat 1) r times with replacement from that original samples $\boldsymbol{x}$ to obtain r bootstrap datasets $\boldsymbol{x}^*=\{\boldsymbol{x}_1^*, \boldsymbol{x}_2^*, \cdots, \boldsymbol{x}_r^*\}$
3) For each bootstrap dataset, estimate the statistic of interest $\theta^*(\boldsymbol{x}_i^*)$, and then a statistic vector $\boldsymbol{\theta}^*=\{\theta^*(\boldsymbol{x}_1^*), \theta^*(\boldsymbol{x}_2^*), \cdots, \theta^*(\boldsymbol{x}_r^*)\}$ is achieved by using the bootstrap resampling;
4) Construct a sampling empirical distribution function (EDF) of $\theta(\boldsymbol{x}^*)$ from the estimated statistic vector $\boldsymbol{\theta}^*$, in which the mean μ^* and standard deviation σ^* in the EDF of $\theta^*(\boldsymbol{x}^*)$ are

$$\begin{cases} \mu^* = \dfrac{\sum_{i=1}^{r} \theta^*\left(\boldsymbol{x}_i^*\right)}{r} \\ \sigma^* = \dfrac{\sum_{i=1}^{r} \left(\theta^*\left(\boldsymbol{x}_i^*\right) - \mu^*\right)^2}{r-1} \end{cases} \tag{8}$$

5) Approximate the mean μ and standard deviation σ in the EDF of $\theta(\boldsymbol{x})$ by using the constructed EDF in step 4).

According to the basic bootstrapping procedure above, it is concluded that applying bootstrap to estimate the distributions of statistics is very convenient. It is a straightforward way to derive standard deviations and CIs of estimators for parameters with complex distribution. Therefore, the bootstrapping has been widely used in the regression model estimation, machine learning, data mining, etc. Due to different goals of application, several types of bootstrap scheme were developed such as bayesian bootstrap, parametric bootstrap, resampling residuals, wild bootstrap, block bootstrap, etc. The bootstrap approach in this work is employed to solve the regression model for the coefficients of hyperplane. Therefore, the bootstrapping regression model is used here and solved by the resampling residuals [28]. Take a simple regression model $y=\alpha+\beta x$ as example, using the residual resampling to estimate CIs around the regression coefficients α and β of the regression model can be briefly summarized below [28], [29], [30]:

1) Estimate initial regression coefficients α_0 and β_0 on the original samples $[\boldsymbol{y}, \ \boldsymbol{x}]$ through $[\alpha_0, \ \beta_0]=\boldsymbol{y}\left([\mathbf{1}, \ \boldsymbol{x}]^T[\mathbf{1}, \ \boldsymbol{x}]\right)^{-1}[\mathbf{1}, \ \boldsymbol{x}]^T$;

2) Use the estimated initial regression model $y=\alpha_0+\beta_0 x$ to calculate the predicted values and residuals where the predicted values $y_i'=\alpha_0+\beta_0 x_i$ and the corresponding residuals $\xi_i = y_i - y_i'$.

3) Formulate the EDF of residuals by using the calculated residuals $\boldsymbol{\xi} = [\xi_1, \ \xi_2, \ \ldots, \ \xi_m]$ where m is the number of original samples.

4) Bootstrap s residuals from the vector of residuals $\boldsymbol{\xi}$ and use these ones to create a bootstrap dataset which contains s synthetic response variable y_i^*s. That is, add a randomly resampled residual ξ_j drawn from the set of residual values $\boldsymbol{\xi}$ to each predicted values y_i', hence, $y_i^* = y_i' + \xi_j$.

5) Regress these bootstrapped $\boldsymbol{y}^*$s on the original $\boldsymbol{x}$ to obtain bootstrap regression coefficients α_k^* and β_k^* through $\left[\alpha_k^*, \ \beta_k^*\right]=\boldsymbol{y}_k^*\left([\mathbf{1}, \ \boldsymbol{x}]^T[\mathbf{1}, \ \boldsymbol{x}]\right)^{-1}[\mathbf{1}, \ \boldsymbol{x}]^T$ with the samples drawn from the bootstrap dataset. For each bootstrap dataset, both coefficients α_k^* and β_k^* are estimated. The values of the estimated regression coefficients α_k^* and β_k^* will be different in each bootstrap iteration but the independent variable observations are unchanged from the original sample.

6) Repeat 4) and 5) with large number of times r, r bootstrap datasets are created. For each bootstrap dataset, the α_k^* and β_k^* are solved. Therefore, for the created r bootstrap datasets, the coefficient vectors of $\boldsymbol{\alpha}^*$ and $\boldsymbol{\beta}^*$, which are $\boldsymbol{\alpha}^*=\left[\alpha_1^*, \ \alpha_2^*, \ \ldots \ \alpha_r^*\right]$ and $\boldsymbol{\beta}^*=\left[\beta_1^*, \ \beta_2^*, \ \ldots \ \beta_r^*\right]$ are obtained respectively.

7) Calculate the bootstrap means and standard deviations of the regression coefficients α^* and β^* via (8) by using the estimated vectors of $\boldsymbol{\alpha}^*$ and $\boldsymbol{\beta}^*$, $\boldsymbol{\alpha}^*=\left[\alpha_1^*,\ \alpha_2^*,\ \cdots\ \alpha_r^*\right]$ and $\boldsymbol{\beta}^*=\left[\beta_1^*,\ \beta_2^*,\ \cdots\ \beta_r^*\right]$.

8) Solve the 95% CIs for the means and standard deviations of the α^* and β^* as:

$$\begin{cases} \mu^*\left(\alpha^*\right)=\left[\alpha^*-t_{r-1,0.25}\dfrac{s\left(\alpha^*\right)}{r},\ \ \alpha^*+t_{r-1,0.25}\dfrac{s\left(\alpha^*\right)}{r}\right] \\ \sigma^*\left(\alpha^*\right)=\left[\sqrt{\dfrac{(r-1)s^2\left(\alpha^*\right)}{\chi^2_{0.025}}},\ \ \sqrt{\dfrac{(r-1)s^2\left(\alpha^*\right)}{\chi^2_{0.975}}}\right] \\ \mu^*\left(\beta^*\right)=\left[\beta^*-t_{r-1,0.25}\dfrac{s\left(\beta^*\right)}{r},\ \ \beta^*+t_{r-1,0.25}\dfrac{s\left(\beta^*\right)}{r}\right] \\ \sigma^*\left(\beta^*\right)=\left[\sqrt{\dfrac{(r-1)s^2\left(\beta^*\right)}{\chi^2_{0.025}}},\ \ \sqrt{\dfrac{(r-1)s^2\left(\beta^*\right)}{\chi^2_{0.975}}}\right] \end{cases} \tag{9}$$

where t is Student's t distribution and χ^2 is chi-squared distribution.

4.2. Bootstrap Based CI Estimation for TSRB

Comparing the bootstrapping regression model above and the hyperplane expressions in (4), it is confirmed that the expression of the TSRB approximation hyperplane is a regression model essentially and the hyperplane coefficients, i.e., the regression coefficients can be solved using the resampling residuals. Apply the bootstrap-based CI approach to estimate coefficients of the TSRB approximation hyperplane, the item in (4) should be rewritten as the following general form

$$\bar{d}_1=\alpha+\beta_1\bar{d}_2+\cdots+\beta_{n-1}\bar{d}_n \tag{10}$$

where $\alpha=i_k^{\max}/\beta_{k,1}$; $\beta_1=-\beta_{k,2}/\beta_{k,1}$ and $\beta_{n-1}=-\beta_{k,n}/\beta_{k,1}$.

Take the $\bar{d}_1$ as the output of the regression model and $\bar{d}_2$, $\bar{d}_3$, ···, and $\bar{d}_n$ as the inputs of the regression model, the $\bar{d}_1=\alpha+\beta_1\bar{d}_2+\cdots+\beta_{n-1}\bar{d}_n$ is indeed a general regression model and the coefficients α, β_1, β_2, ···, and β_{n-1} in (10) can be hence solved by the bootstrap based CI estimation approach. Following the procedure of the bootstrap based CI estimation approach for bootstrapping regression model in section 4.1, given a set of TSRB points $\bar{\boldsymbol{D}}_k=\left[\bar{\boldsymbol{d}}_{k,1},\bar{\boldsymbol{d}}_{k,2},\cdots,\bar{\boldsymbol{d}}_{k,i}\right]$ with respect to the thermal constraint of the kth branch, the bootstrap based CI estimation for the coefficients of hyperplane approximating TSRB with respect to the thermal constraint of the kth branch can be described as follows.

1) Estimate the initial coefficients of hyperplane α_0, $\beta_{1,0}$, $\beta_{2,0}$, ···, $\beta_{n-1,0}$ via $[\alpha_0,\ \beta_{1,0},\ \cdots,\ \beta_{n-1,0}]=\bar{\boldsymbol{d}}_{k1}\left(\bar{\boldsymbol{d}}_k^T\bar{\boldsymbol{d}}_k\right)^{-1}\bar{\boldsymbol{d}}_k^T$ in which $\bar{\boldsymbol{d}}_k=\left[\mathbf{1},\bar{\boldsymbol{d}}_{k,2},\bar{\boldsymbol{d}}_{k,3},\cdots,\bar{\boldsymbol{d}}_{k,i}\right]^T$ by using the given set of TSRB points $\bar{\boldsymbol{D}}_k=\left[\bar{\boldsymbol{d}}_{k,1},\bar{\boldsymbol{d}}_{k,2},\cdots,\bar{\boldsymbol{d}}_{k,i}\right]$.

2) Pass the original TSRB points $\bar{\boldsymbol{D}}_k=\left[\bar{\boldsymbol{d}}_{k,1},\bar{\boldsymbol{d}}_{k,2},\cdots,\bar{\boldsymbol{d}}_{k,i}\right]$ through the initial hyperplane model $\bar{d}_1'=\alpha_0+\beta_{1,0}\bar{d}_2+\cdots+\beta_{n-1,0}\bar{d}_n$ to generate the predicted values $\bar{d}_1'$.

3) Calculate the hyperplane residuals ξs via $\xi_i = \bar{d}_{1,i} - \bar{d}_{1,i}'$ by using the original $\bar{d}_1$ and the predicted values $\bar{d}_1'$.

4) Formulate the EDF of residuals by using the estimated residuals ξ.

5) Regenerate s residual samples ξ_js from the estimated EDF of ξ, and add these resampled residuals ξ_js randomly drawn from the set of residual values ξ to the predicted values $\bar{d}_1'$ to create a bootstrap dataset $\bar{d}_{1i}^*$ which contains s synthetic response variables $\bar{d}_{1i}^* = \bar{d}_{1i}' + \xi_j$.

6) Regress the bootstrapped $\bar{d}_{1i}^*$ on the fixed $\bar{d}_k = \left[\mathbf{1}, \bar{d}_{k,2}, \bar{d}_{k,3}, \cdots, \bar{d}_{k,i}\right]^T$, the hyperplane coefficients α^*, β_1^*, ···, and β_{n-1}^* are estimated via $\left[\alpha^*, \ \beta_1^*, \ \cdots, \ \beta_{n-1}^*\right] = \bar{d}_{k1}^* \left(\bar{d}_k^T \bar{d}_k\right)^{-1} \bar{d}_k^T$.

7) Repeat 5) and 6) r times, r bootstrap datasets are created. For each bootstrap dataset, the hyperplane coefficients α^*, β_1^*, ···, and β_{n-1}^* are all estimated. Finally, the hyperplane coefficients vectors $\boldsymbol{\alpha}^* = \left[\alpha_1^*, \ \alpha_2^*, \ \cdots \ \alpha_r^*\right]$, $\boldsymbol{\beta}_1^* = \left[\beta_{1,1}^*, \ \beta_{1,2}^*, \ \cdots \ \beta_{1,r}^*\right]$, ···, and $\boldsymbol{\beta}_{n-1}^* = \left[\beta_{n-1,1}^*, \ \beta_{n-1,2}^*, \ \cdots \ \beta_{n-1,r}^*\right]$ are achieved.

8) For each hyperplane coefficient vector, calculate there EDF of the hyperplane coefficient via (8), hence, the means and standard deviations for the bootstrapped coefficient parameters $\left[\alpha^*, \ \beta_1^*, \ \cdots, \ \beta_{n-1}^*\right]$ are obtained.

9) Calculate the CIs of the means and standard deviations for the hyperplane coefficients α^*, β_1^*, ···, and β_{n-1}^* through (9) based on the EDF.

10) Approximate the means μs and standard deviations σs in the EDFs of α, β_1, β_2, ···, and β_{n-1} by using the constructed EDF and CIs in 8) and 9)

It should be noted that the residual sampling is a model-dependent method which means the estimation results are subject to the initial estimated regression model. Big errors in the initial estimated model might affect the CI estimation significantly. Therefore, the CI estimation must be interpreted properly.

5. Case study

In this section, the China Southern Power Grid (CSG) is used as a benchmark to evaluate the performance of proposed approach for TSRB approximation. CSG, as shown in Fig.2, is one of the largest AC/DC hybrid transmission systems in China. It includes the power networks throughout Guangdong (GD), Guangxi (GX), Yunnan (YN), Guizhou (GZ) and Hainan (HN) provinces with a total service area spanning 1 million square kilometers and a population of 252 million. In CSG, most of power generated in YN, GZ and GX is transmitted to the load center in the GD through AC/DC parallel ties over 1,000 kilometers. The transmission corridors from west to east consist of 10 HVDC links and 8 AC interties. Years of operation experiences indicate that

the thermal security of AC interties seriously threatens the operation security of CSG with inter-area oscillations and multiple HVDCs blocking simultaneously [26].

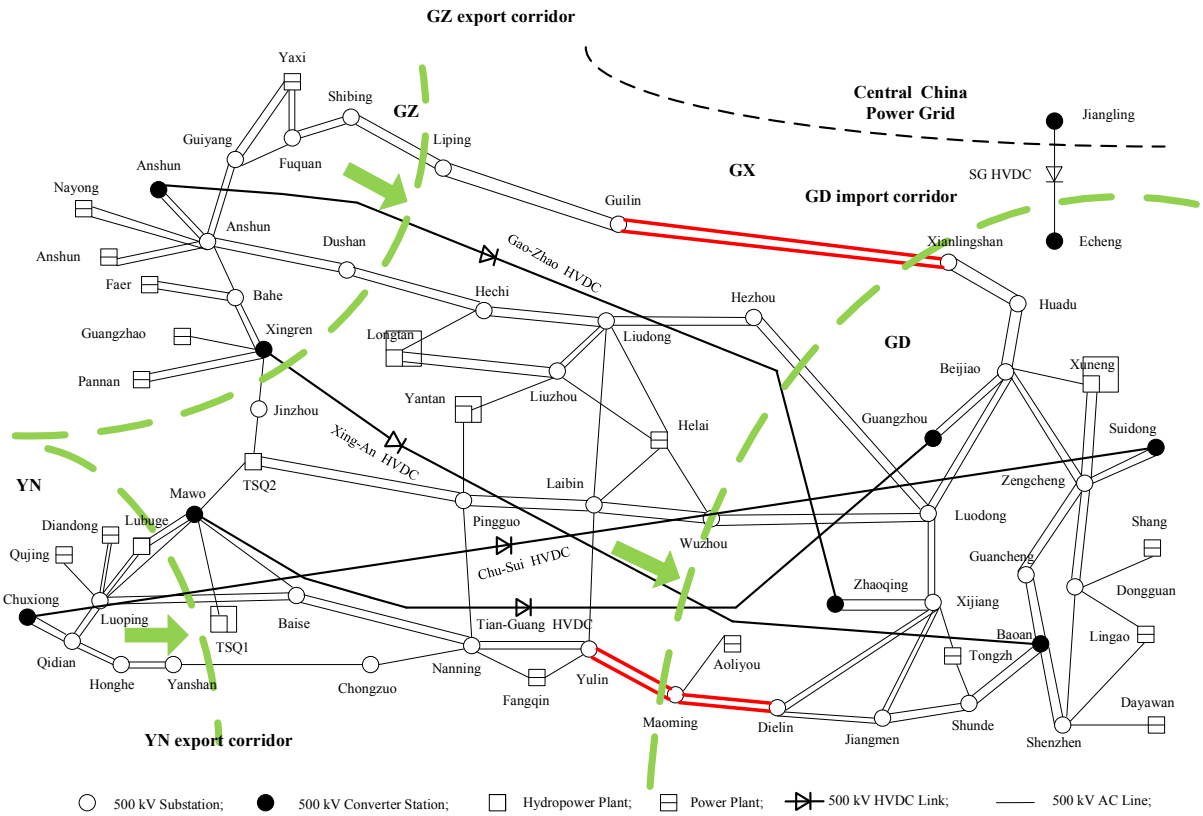

Fig.2 Scheme of CSG

To facilitate the situational awareness of CSG in thermal security, the TSR of CSG with *N*-1 contingency is developed in this section using the proposed approach. Although there are more than thousands of branches in CSG, the thermal security of interties dominates the thermal security of CSG. Hence, the TSR of CSG developed in this work will focus on the interties which interconnect the provincial power grids in CSG. According to the AC corridor partition in CSG and the historical experience of operation, the interties Yulin-Maoming (YM), Maoming-Dielin (MD) and Guilin-Xinlinshan (GS) on the AC import corridor of GD are subject to thermal violations due to the operating alternations. Note that YM and MD locate in the southern import corridor of GD while GS is in the northern import corridor of GD. In this section, the TSR of CSG with respect to the thermal constraints of YM, MD and GS are developed. The descriptor variable d_1 in this TSR is selected as the total active power on the AC import corridor of GD, and the descriptor variables d_2 and d_3 are selected as the injected active power from buses which significantly influence the power flow on the interties YM, MD and GS.

5.1. TSR with respect to thermal constraint of YM

In this section, the TSR with respect to thermal constraint of YM considering *N*-1 contingency is investigated. According to the CSG operational experiences and security analysis, the injected active power of PV bus YX and TS influence the power flow on YM significantly. Therefore, the descriptor variables d_1, d_2 and d_3 in this TSR are selected as the total active power on AC corridor

of GD, active power injections on bus YX and TS, respectively. For the studied interties and the determined descriptor variables, 60 TSRB points with respect to thermal constraint of YM are tracked via RPF with different stress directions. Using the these 60 TSRB points as original dataset $\bar{\boldsymbol{D}}_k$, an initial hyperplane expression (also named regression model) $d_1=\alpha_0+\beta_{1,0}d_2+\beta_{2,0}d_3$ is solved through LSE, where α_0=9343.7499, $\beta_{1,0}$=0.3224 and $\beta_{2,0}$=0.9135.

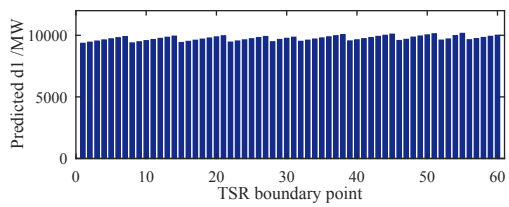

Fig.3 d1 predicted by initial hyperplane expression

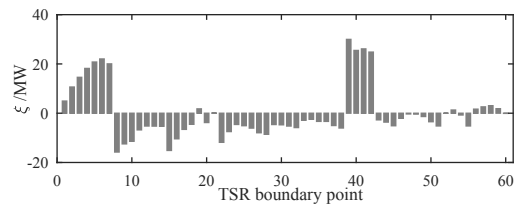

Fig.4 Residuals calculated by initial hyperplane expression

Pass the original d_2 and d_3 to the solved hyperplane expression, a series predicted d_1' is obtained and shown in Fig.3. Comparing the predicted d_1' with the original d_1, the residuals ξ are calculated via step 3) in section 4.2 and shown in Fig.4. Randomly bootstrap s residuals from the calculated residuals ξ with replacement to create synthetic d_1^*, a bootstrap dataset $\boldsymbol{d}_{1,k}^*$ is obtained. Here, s is set to be the number of the original TSRB points. Hence, the number of synthetic d_1^* in $\boldsymbol{d}_{1,k}^*$ is s. Regress these bootstrapped d_1^* in $\boldsymbol{d}_{1,k}^*$ on the original d_2 and d_3, the statistics α_k^*, $\beta_{1,k}^*$ and $\beta_{2,k}^*$ are calculated via step 6) in section 4.2. Following step 7) in section 4.2, repeat above process r times where the r is set to be 100000, 10000 bootstrap datasets are achieved. For each achieved bootstrap dataset $\boldsymbol{d}_{1,k}^*$, regress the synthetic d_1^*s in $\boldsymbol{d}_{1,k}^*$ on the original d_2 and d_3, the α_k^*, $\beta_{1,k}^*$ and $\beta_{2,k}^*$ are all estimated. Therefore, estimated hyperplane coefficients vectors $\boldsymbol{\alpha}^*=\left[\alpha_1^*,\ \alpha_2^*,\ \cdots\ \alpha_{100000}^*\right]$, $\boldsymbol{\beta}_1^*=\left[\beta_{1,1}^*,\ \beta_{1,2}^*,\ \cdots\ \beta_{1,100000}^*\right]$ and $\boldsymbol{\beta}_2^*=\left[\beta_{2,1}^*,\ \beta_{2,2}^*,\ \cdots\ \beta_{2,100000}^*\right]$ are obtained.

Table 1 EDFs of coefficients and computational times compared with different samples

TSRB with respect to Intertie	Coefficient of hyperplane	mean	CI for mean		Std	CI for Std	
YM	α	9343.7427	[9343.7289,	9343.7562]	3.1172	[3.1083,	3.1276]
	β_1	0.3224	[0.3223,	0.3224]	0.0047	[0.0046,	0.0047]
	β_2	0.9135	[0.9135,	0.9136]	0.0068	[0.0067,	0.0068]

For the obtained coefficients vectors $\boldsymbol{\alpha}^*$, $\boldsymbol{\beta}_1^*$ and $\boldsymbol{\beta}_2^*$, the means and standard deviations of α^*, β_1^* and β_2^*, as well as their CIs are estimated through steps 8 and 9 in section 4.2, and the results are listed in Table 1. It is clear that the means of α^*, β_1^* and β_2^* fluctuate around 9343.7427, 0.3224 and 0.9135 with narrow Cis, respectively, and the standard deviations of α^*, β_1^* and β_2^* are also around 3.1172, 0.0047 and 0.0068 with narrow Cis, respectively. Based on the narrow CIs of means and small standard deviations, accuracy of the estimated coefficients for the TSRB approximation hyperplane could be validated. Moreover, the narrow CIs also demonstrate that the proposed bootstrap based CI estimation performs with high quality and reliability for the estimated coefficients of TSRB approximation hyperplane.

In the aid of the estimated means and standard deviations of α^*, β_1^* and β_2^* in Table 1, the EDFs of α^*, β_1^* and β_2^* are obtained as $\alpha^* \sim \boldsymbol{N}(9343.7426, 3.1171^2)$, $\beta_1^* \sim \boldsymbol{N}(0.3223, 0.0047^2)$ and $\beta_2^* \sim \boldsymbol{N}(0.9135, 0.0068^2)$, respectively. Hence, the EDFs for the coefficients of the TSRB approximation hyperplane are $\alpha_1 \sim \boldsymbol{N}(9343.7632, 3.1233^2)$, $\beta_1 \sim \boldsymbol{N}(0.3223, 0.0047^2)$ and $\beta_2 \sim \boldsymbol{N}(0.9135, 0.0068^2)$. According to estimated EDFs of the coefficients of the hyperplane, it is obtained that the expression of the hyperplane approximating the TSR with respect to the YM with N-1 contingency is d_1=9343.7426+3.1171d_2+0.9135d_3. Using the estimated expression of the hyperplane, the TSRB with respect to the thermal constraint of YM is approximated and shown in Fig.5. As can be seen, almost all the TSRB points are on the approximation hyperplane, which demonstrates that the estimated hyperplane performs a good fitting for the TSRB.

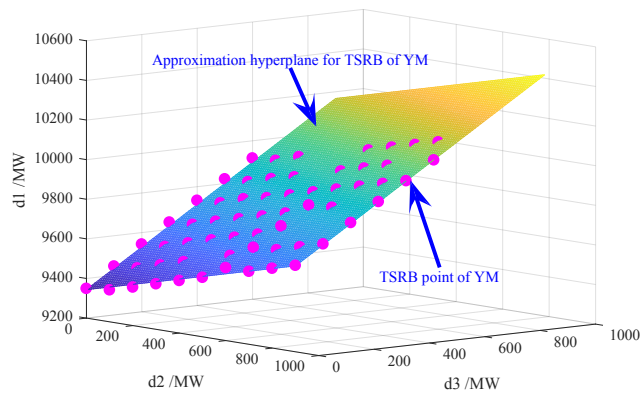

Fig.5 TSRB with respect to YM approximated by the estimated hyperplane

To further evaluate the approximation accuracy of the proposed approach quantitatively, Fig.6 scatters all the predicted d_1 on the two-dimensional active power space with predicted d_1 and actual d_1 as axis. It is obvious that the predicted d_1 matches the actual d_1 very well. Fig.7 further shows the residuals between the predicted d_1 and actual d_1. As can be seen, the maximum and average residuals among the calculated residuals in Fig.7 is 30.0068MW and 7.6152MW, while their corresponding relative maximum and average errors are 0.3211% and 0.0805%, respectively. Through the comparisons and discussion above, it is concluded the hyperplane estimated via the proposed bootstrap based CI approach can approximate the TSRB precisely.

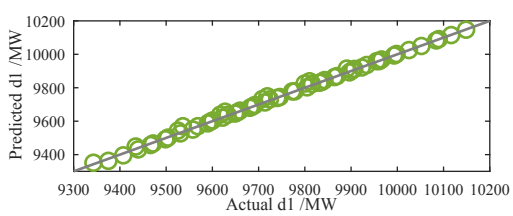

Fig.6 Predicted and actual d1 comparison

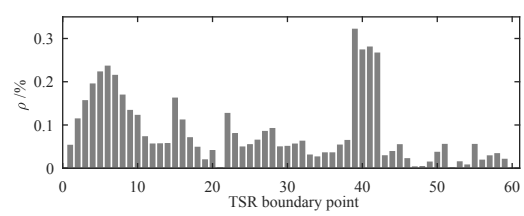

Fig.7 residuals of TSRB with respect to YM

5.2. Choice of repetition times

As mentioned above, the repetition times r in the bootstrap based CI estimation significantly influence the approximation accuracy. In order to achieve the more accurate EDF of statistic, a large number of bootstrap datasets r is required. There is a

tradeoff between the estimation accuracy and computational efficiency. The larger number of bootstrap datasets drawn, the more computational time cost, and vice versa. Hence, the influences of the repetition times on the approximated results are discussed in this section to facilitate the selection of appropriate values to balance the approximation accuracy and computational efficiency.

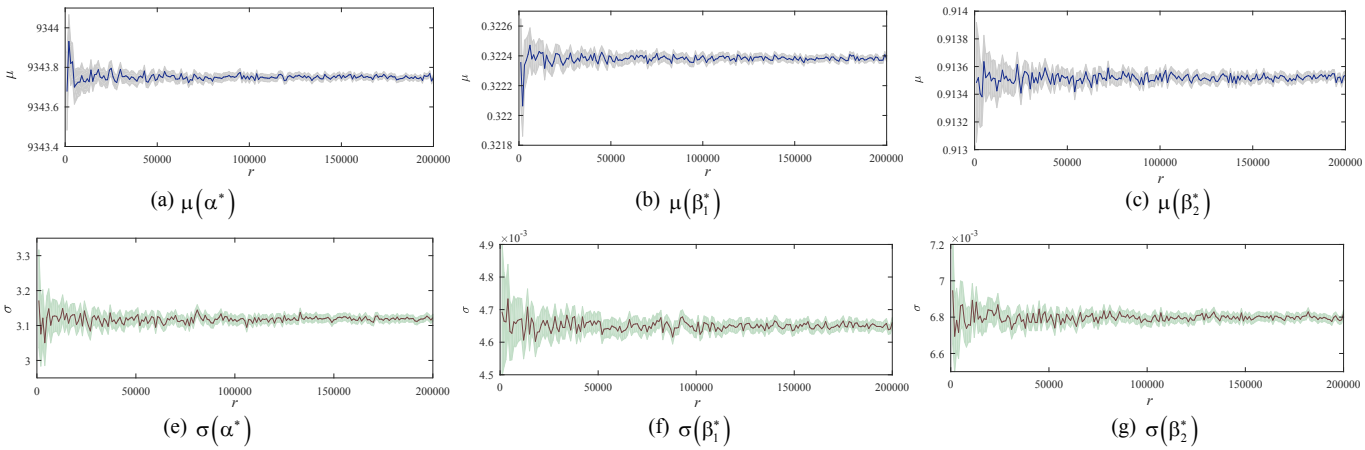

Fig.8 EDFs of coefficients for approximation hyperplane estimated with different repetition times

As described in procedure of the bootstrap based CI estimation in section 4.2, Fig.8 illustrates the estimated EDFs of coefficients of the approximation hyperplane as well as their CIs with the drawn 60 samples for each bootstrap dataset and the repetition times *r* to create the number of bootstrap datasets increasing from 1,000 to 200000 by the proposed bootstrap based CI estimation. It is clear from Fig.8 that, for the EDF of α^*, the CIs of $\mu*$ and $\sigma*$ range from [9343.4835, 9343.8769] and [3.0372, 3.3157] with 1000 bootstrap datasets to [9343.7371, 9343.7645] and [3.1129, 3.1322] with 200000 bootstrap datasets, respectively. For the EDF of β_1^*, the CIs of the mean $\mu*$ and standard deviation $\sigma*$ range from [0.3221, 0.3226] and [0.0045, 0.0049] with 1000 bootstrap datasets to [0.3223, 0.3224] and [0.0046, 0.0046] with 200000 bootstrap datasets respectively. For the EDF of β_2^*, the CIs of $\mu*$ and $\sigma*$ range from [0.9131, 0.9139] and [0.0067, 0.0072] with 1000 bootstrap datasets to [0.9135, 0.9136] and [0.0067, 0.0068] with 200000 bootstrap datasets respectively. Comparing the trends on the estimated CIs of the mean $\mu*$s and standard deviation $\sigma*$s for the α^*, β_1^* and β_2^* with bootstrap datasets increasing in Fig.8, it is found that ranges of the CIs for the mean $\mu*$s and standard deviation $\sigma*$s of the α^*, β_1^* and β_2^* are shrinking to almost constant ranges with the bootstrap datasets increasing. This is inferred that the more bootstrap datasets drawn in the procedure of the proposed bootstrap based CI estimation, the more accurate EDFs of α^*, β_1^* and β_2^* estimated. However, the more bootstrap datasets drawn, the more computational time costs.

Table 2 Computational time and EDFs of coefficients compared with different repetition times

r	EDF of α^*		EDF of β_1^*		EDF of β_2^*		Computational time /s
	$\mu(\alpha^*)$	$\sigma(\alpha^*)$	$\mu(\beta_1^*)$	$\sigma(\beta_1^*)$	$\mu(\beta_2^*)$	$\sigma(\beta_2^*)$	
1000	9343.7397	3.0327	0.3224	0.0048	0.9134	0.0066	0.1738
2000	9343.8348	3.1753	0.3223	0.0047	0.9134	0.0068	0.3271
5000	9343.7958	3.1125	0.3223	0.0047	0.9135	0.0068	0.7759
8000	9343.8028	3.1326	0.3223	0.0046	0.9134	0.0069	1.0918
10000	9343.8300	3.1219	0.3222	0.0047	0.9135	0.0068	1.3764
50000	9343.7917	3.1261	0.3223	0.0047	0.9135	0.0068	6.8254
100000	9343.7759	3.1069	0.3223	0.0047	0.9135	0.0068	12.9190

150000	9343.7922	3.1117	0.3223	0.0047	0.9135	0.0068	19.3382
200000	9343.7817	3.1095	0.3223	0.0047	0.9135	0.0068	25.3918

The estimated results and the computational time with different bootstrap datasets are compared in Table 2. It is obvious that the EDFs of the α^*, β_1^* and β_2^* are slightly influenced by the number of bootstrap datasets, while the computational times are significantly increased from 0.1738s with 1000 bootstrap datasets to 25.3918s with 200000 bootstrap datasets. Note that the CIs for the EDFs of the α^*, β_1^* and β_2^* in Fig.8 are decreased with the number of bootstrap datasets increasing, and the shrunk CIs mean higher quality and reliability of the estimated results. Comparing the trends on estimated CIs of EDFs, it can be seen that the ranges for the CIs are almost constant with the number of bootstrap datasets greater than 100000. Therefore, considering the estimation accuracy, reliability and computational efficiency in the proposed approach, the number of repetition times *r* is set to be 100000 in this work.

Table 3 EDFs and CIs for the coefficients of hyperplanes approximating TSRB with respect to YM and MD

Number of hyperplanes	TSRB with respect to Intertie	Coefficient	mean	CI for mean	Std	CI for Std
1	YM and MD	α	9466.6411	[9466.4831, 9466.7992]	36.0632	[35.9518, 36.1753]
		β_1	0.2966	[0.2881, 0.3051]	0.0548	[0.0545, 0.0549]
		β_2	0.4409	[0.4407, 0.4412]	0.0526	[0.0525, 0.0528]
2	YM	α	9343.7427	[9343.7289, 9343.7562]	3.1172	[3.1083, 3.1276]
		β_1	0.3224	[0.3223, 0.3224]	0.0047	[0.0046, 0.0047]
		β_2	0.9135	[0.9135, 0.9136]	0.0068	[0.0067, 0.0068]
	MD	α	11380.3234	[11380.2436, 11380.4033]	2.2203	[2.1640, 2.2770]
		β_1	0.3708	[0.3707, 0.3708]	0.0078	[0.0077, 0.0078]
		β_2	-2.0394	[-2.0395, -2.0393]	0.0228	[0.0227, 0.02229]

5.3. TSRB with respect to thermal constraints of YM and MD

The performance of the proposed approach evaluated in section 5.2 proves that the proposed approach can estimate an appropriate hyperplane to approximate the TSRB with respect to thermal constraint of one intertie precisely. In this section, the proposed approach is used to approximate the TSRB with respect to thermal constraint of multiple interties. The CSG operation reports point out that the injected active power at bus YX and TS significantly affects the power flow on intertie MD which may violate the thermal constraint with *N*-1 contingency in CSG. Hence, with the same descriptor variables in Fig.5, the TSRB with respect to thermal constraints of YM and MD is approximated by the proposed approach. The original TSRB points with respect to these two interties with *N*-1 contingency are tracked by RPF and shown in Fig.9(a). First, one hyperplane is employed to approximate the TSRB with respect to these two interties. The EDFs of the coefficients for the hyperplane approximating TSRB with respect to YM and MD are estimated and shown in Table 3. Although the expression of TSRB approximation hyperplane, i.e., d_1= 9466.6411+ 0.2966d_2+ 0.4409d_3, can be obtained using the estimated EDFs of coefficients in Table 3, the standard deviations for the estimated coefficients α^*, β_1^* and β_2^* are very large. Particularly, the standard deviation of α^* is 36.0632. From the estimated standard deviations and CIs in Table 3, it can be inferred that the estimated hyperplane has very poor approximation for the TSRB with respect to YM and MD.

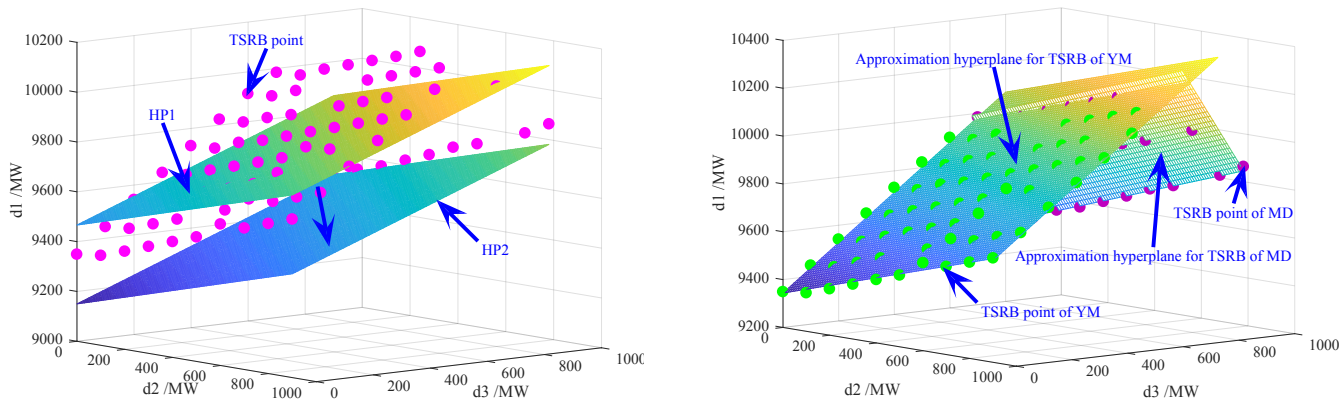

(a)TSR approximated by one hyperplane (b) TSR approximated by two hyperplanes

Fig.9 TSR with respect to YM and MD

Fig.9(a) shows the obtained TSR with the boundary approximated by the estimated hyperplane HP1. It is obvious that hyperplane HP1 cannot fit the TSRB very well. Only very few original TSRB points are on HP1, and the rest ones are far from HP1. Using this TSR to evaluate the thermal security of the AC import corridor of GD will bring a lot of thermal insecure operation points into the TSR and exclude some secure operation points from the TSR. To cope with this issue, the general approach is to shift the approximation hyperplane from HP1 to HP2 as shown in Fig.9(a). Although this shifting approach can filter out all the thermal insecure operation points from the TSR, there are a few thermal secure operation points are separated into the thermal insecure region (TISR). As a result, false alarms will appear in the power grid thermal security monitoring.

To address the above issue, the TSRB corresponding to thermal constraint of each intertie is approximated by one hyperplane. Thus, the intersection of all TSRs is the TSR with respect to all considered interties, i.e., YM and MD. Hence, the EDFs of the coefficients for the hyperplanes approximating TSRBs with respect to YM and MD are estimated via the proposed method respectively. The results are shown in Table 3. As can be seen, the approximation hyperplane of TSRB with respect to YM is d_1=9343.7427+0.3224d_2 +0.9135d_3, and the approximation hyperplane of TSRB with respect to MD is d_1=11380.3234+0.3708d_2–2.0394d_3. The standard deviations and CIs for the estimated coefficients α^*, β_1^* and β_2^* of these two hyperplanes are also listed in Table 3. Comparing the standard deviations and CIs for the estimated coefficients α^*, β_1^* and β_2^* of the approximation hyperplanes in Table 3, it can be found that standard deviations and CI intervals for the estimated coefficients α^*, β_1^* and β_2^* decrease from one hyperplane approximating TSRB to two hyperplane rapidly. In particular, the standard deviation of α^* decreases from 36.0632 with one approximation hyperplane to 3.1172 and 2.2203 with two one approximation hyperplanes. This indicates that TSRB with respect to each intertie approximated by one hyperplane can improve the approximation precision of TSRB. Correspondingly, the TSRB with respect to YM and MD using two hyperplanes is approximated and shown in Fig.9(b). Comparing the approximation hyperplane in Fig. 9, it is obvious that the hyperplanes in Fig.9(b) better fits for the TSRB with respect to the thermal constraints of YM and MD.

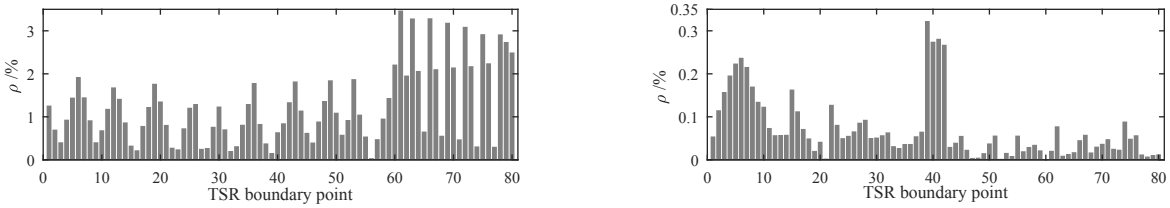

(a) One hyperplane approximating TSRB (b) Two hyperplanes approximating TSRB

Fig.10 Residuals of the TSRB with respect to YM and MD

To quantitatively compare the precision of the approximation in Fig.9, Fig.10 represents the calculated relative errors of Fig.9. As can be seen, using one hyperplane to approximate the TSRB with respect to YM and MD can cause big errors and the maximum relative error is 3.4566%, while using two hyperplanes to approximate this TSRB can improve the approximation accuracy significantly and the maximum relative error is only 0.3211%. This confirms that the TSRB with respect to each intertie requires to be approximated by at least one hyperplane. More interties considered in the TSR, more approximation hyperplanes are required.

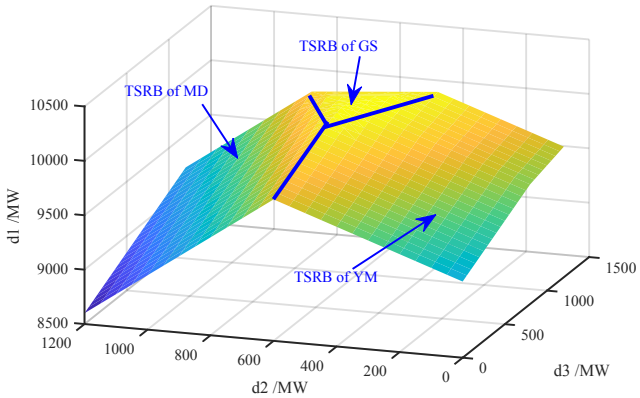

Fig.11 TSR with respect to YM, MD and GS

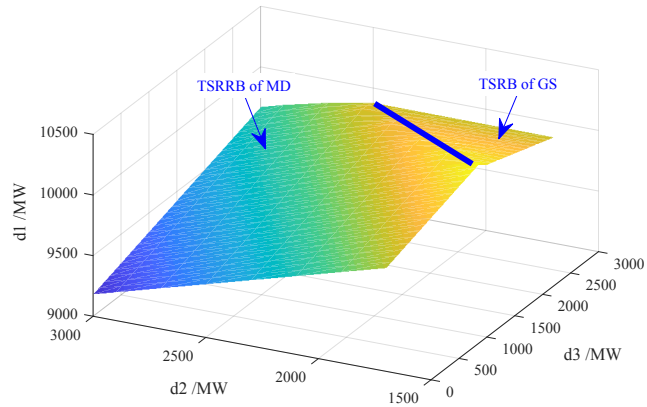

Fig.12 TSR with respect to MD and GS

5.4. *Application of TSR in CSG*

The representations above not only confirm that the proposed bootstrap based CI estimation can accurately estimate the coefficients of hyperplane which can approximate TSRB precisely, but also verify the TSRB with respect to the thermal constraints of one intertie requires at least one hyperplane to approximate. In this section, the proposed approach is further employed to construct the TSR of CSG with respect to the thermal constraints of multiple interties to monitor the thermal security of the interties on the AC import corridor of GD. On AC import corridor of GD, beyond MD and YM, the GS which is part of the north AC import corridor of GD also may violate the thermal constraint with *N*-1 contingency because of CSG operation pattern. The security analysis and operation experience of CSG reveal that the power flow on YM, MD and GS are all significantly influenced by the active power injection from buses YX and TS, moreover, the power flow on MD and GS are also significantly affected by the active power injection from buses GPT and QBF. Hence, it is obvious that two TSRs should be formed to monitor the thermal security of the interties on the AC import corridor of GD in CSG. Referring to the previous choice of descriptor variables, for the former one, the total active power on AC import corridor of GD and active power injections from buses YX and TS are determined as the descriptor variables d_1, d_2 and d_3 respectively to construct the TSR with respect to YM, MD and GS. For the latter one, the

total active power on AC import corridor of GD and active power injections from buses GPT and QBF are selected as the descriptor variables d_1, d_2 and d_3 respectively to form the TSR with respect to MD and GS

Table 4 EDFs for the coefficients of hyperplanes approximating TSRB with respect to YM, MD and GS

TSRB with respect to Intertie	Coefficient of hyperplane	mean	CI for mean	Std	CI for Std
YM	α	9343.7426	[9343.2517, 9344.1933]	3.1172	[2.8315, 3.4692]
	β_1	0.3223	[0.3217, 0.3230]	0.0047	[0.0042, 0.0051]
	β_2	0.9135	[0.9125, 0.9146]	0.0068	[0.0061, 0.0076]
MD	α	11380.3234	[11377.5551, 11383.0832]	5.2147	[4.3383, 5.3581]
	β_1	0.3708	[0.3697, 0.3721]	0.0077	[0.0069, 0.0087]
	β_2	-2.0394	[-2.0428, -2.0360]	0.0228	[0.0202, 0.0255]
GS	α	10352.6275	[10351.8803, 10353.3229]	5.0804	[4.6290, 5.6036]
	β_1	-0.1184	[-0.1190, -0.1179]	0.0037	[0.0034, 0.0040]
	β_2	-0.2500	[-0.2508, -0.2492]	0.0057	[0.0053, 0.0064]

Following the proposed procedure above, the coefficients of the hyperplanes approximating boundaries of TSR are solved. For the TSR with respect to interties YM, MD and GS with the descriptor variables as total active power on AC import corridor of GD and active power injections from buses YX and TS, Table 4 lists the estimated EDFs for the coefficients of the hyperplanes approximating the TSRB with respect to these three interties. The expressions of the three hyperplanes approximating TSRB with respect to interties YM, MD and GS are d_1=9343.7426+0.3223d_2+0.9135d_3, d_1=11380.3705+0.3708d_2–2.0394d_3 and d_1=10352.6275–0.1184d_2–0.2500d_3, respectively. Moreover, the approximation quality and reliability are evaluated by using the estimated standard deviations and CIs in Table 4. It can be concluded that the estimated hyperplanes can fit the TSRB with respect to TM, MD and GS very well. The corresponding TSR are approximated and shown in Fig.11.

Table 5 EDFs and CIs for the coefficients of hyperplanes approximating TSRB with respect to MD and GS

TSRB with respect to Intertie	Coefficient of hyperplane	mean	CI for mean	Std	CI for Std
MD	α	11380.3234	[11377.5551, 11383.0832]	4.2147	[3.3383, 4.3581]
	β_1	0.3708	[0.3697, 0.3721]	0.0077	[0.0069, 0.0087]
	β_2	-2.0394	[-2.0428, -2.0360]	0.0228	[0.0202, 0.0255]
GS	α	10019.3420	[10014.3396, 10024.8030]	2.6972	[2.4235, 3.0424]
	β_1	0.2208	[0.2149, 0.2273]	0.0399	[0.0362, 0.0449]
	β_2	-0.2646	[-0.2721, -0.2577]	0.0488	[0.0431, 0.0549]

For the TSR with respect to interties MD and GS, and the descriptor variables as total active power on AC import corridor of GD and active power injections from buses GPT and QBF, Table 5 lists the estimated EDFs for the coefficients of the hyperplanes approximating the TSRB with respect to these two interties. It is indicated from Table 5 that, the expressions of the two hyperplanes approximating TSRB with respect to interties MD and GS are d_1=13443.9662−3.4791d_2–0.6799d_3 and d_1= 10019.3420+ 0.2208d_2–0.2646d, respectively. Moreover, it is obtained from the estimated standard deviations and CIs in Table 6 that the estimated hyperplanes can perform a good approximation for the TSRB with respect to MD and GS very well. Using these estimated hyperplanes, the corresponding TSR are approximated and finally shown in Fig.12.

Through the represented case studies for approximating thermal security region of China Southern Power Grid by using the proposed approach Bootstrap-based confidence interval estimation above, the advantages of the proposed approach over the existing method for building the thermal security region in bulk power grids can be concluded as follows

1) The approximation hyperplane, which is estimated by the proposed Bootstrap-based confidence interval estimation, exhibits a good performance to fit the TSRB precisely in bulk power grid validated by the above case studies.

2) The proposed Bootstrap-based CI estimation can significantly improve the computational efficiency of the TSRB approximation by using the residual resampling bootstrap method to create synthetic TSRB points rather than tracking TSRB points by RPF or OPF

3) The TSRB, corresponding to a thermal security limit of a certain intertie with N-1 contingency, should be approximated by one or several hyperplanes. For more thermal security limits of interties, the more hyperplanes are needed to approximate the TSRB.

4) Comparing the existing methods for estimating the hyperplanes to approximate the boundary of thermal security region in bulk power grids, the proposed approach can realize to evaluate the quality and reliability of the TSRB approximation results by using the estimated standard deviations and CIs for the coefficients of TSRB approximation hyperplanes.

5) The proposed Bootstrap-based CI estimation can be used to build the TSR of practical power grid with high penetration of intermittent renewable energy to strengthen the situational awareness of power system in thermal security monitoring and control.

6. Conclusion

A bootstrap based CI estimation approach is developed in this paper to estimate the coefficients of hyperplanes approximating the thermal security region boundary with *N*-1 contingency in bulk power grid and improve the situational awareness in power system thermal security monitoring and control. The proposed method uses the original tracked thermal security region boundary points to estimate the coefficients of the TSRB approximation hyperplane by approximating the distributions of the hyperplane coefficients through the random sampling with replacement. In departure from the previous region boundary approximation methods as a point estimation method, this work further employs standard deviations and CIs of the estimated hyperplane coefficients to measure the quality and reliability of the estimate results. Results of simulation on the CSG prove that the proposed method can obtain hyperplanes to fit the TSRB accurately and show great prospect of practical application in bulk power grid.

Acknowledgement

The authors would like to acknowledge the support in part by National Natural Science Foundation of China (No. 51607033, 51877033 and 51607034), National Key Research and Development Program of China (2016YFB0900903) and International Clean Energy Talent Programme (iCET) of China Scholarship Council.

References

[1] Jin CL, Lu N, Lu S, *et al*. A coordinating algorithm for dispatching regulation services between slow and fast power regulating resources. IEEE Transactions on Smart Grid, 2014; 5(2): 1043-1050.

[2] Makarov YV, Du PW, Pai MA, *et al*. Calculating individual resources variability and uncertainty factors based on their

contributions to the overall system balancing needs. IEEE Transactions on Sustainable Energy, 2014; 5(1): 323-331.

[3] Makarov YV., Du PW, Lu S, *et al*. Wide area power system security region. Pacific Northwest National Laboratory, Richland, WA, PNNL-19063, 2009.

[4] Makarov YV, Du PW, Lu S, *et al*. PMU-based wide-area security assessment: concept, method, and implementation. IEEE Transactions on Smart Grid, 2012; 3(3): 1325-1332.

[5] Wu F, Kumagai S. Steady-state security regions of power systems. IEEE Trans. Circuits Syst., 1982; 29(11): 703–711.

[6] Kaye R, Wu F. Dynamic security regions of power systems. IEEE Trans. Circuits Syst., 1982; 29(9): 612–623.

[7] McCalley JD, Wang S, Zhao QL, *et al*. Security boundary visualization for systems operation. IEEE Trans. Power Syst., 1997; 12(2): 940–947.

[8] Gu X, Canizares CA. Fast prediction of loadability margins using neural networks to approximate security boundaries of power systems. IET Gener. Transm. Distrib. 2007; 1(3): 466–475.

[9] Xiao J, Zu GQ, Gong XX, *et al*. Observation of security region boundary for smart distribution grid. IEEE Transactions on Smart Grid, 2017; 8(4): 1731-1738.

[10] Chen SJ, Chen QX, Xia Q, *et al*. Steady-state security assessment method based on distance to security region boundaries. IET Generation Transmission & Distribution, 2013; 7(3): 288-297.

[11] Yu YX. Security region of bulk power system. International Conference on Power System Technology, Kunming, China, 2002; 1: 13–17.

[12] Su JF, Yu YX, Jia HJ, *et al*. Visualization of voltage stability region of bulk power system. International Conference on. Power System Technology, Kunming, China, 2002; 3: 1665–1668.

[13] Yu YX., Li HL, Han Q., *et al*. Practical boundary of static voltage stability region in cut-set complex power space of power systems. 2005 IEEE/PES Transmission & Distribution Conference & Exposition: Asia and Pacific, Dalian, China, 2005; 1–6.

[14] Myska D. Allocation algorithm review. In Proc. 2nd Workshop Market Participants, Central Allocation Office GmbH, Munich, Germany, 2009. Available: http://central-ao.com/index.php?option=com_content&view=category&layout=blog&id=51&Itemid=114.

[15] Efron B. Tibshirani R. Bootstrap methods: another look at the jackknife. Ann. Statist., 1979; 7(1): 1–26.

[16] Wei JQ, Li GY, Zhou M. Monte Carlo simulation and bootstrap method based assessment of available transfer capability in AC–DC hybrid systems. International Journal of Electrical Power & Energy Systems, 2013; 53: 231-236.

[17] Anderson MG., Zhou N, Pierre JW., *et al*. Bootstrap-based confidence interval estimates for electromechanical modes from multiple output analysis of measured ambient data. IEEE Transactions on Power Systems, 2005; 20(2): 943-950.

[18] Tahir MF, Tehzeeb-ul-Hassan, Saqib MA. Optimal scheduling of electrical power in energy-deficient scenarios using

artificial neural network and bootstrap aggregating. International Journal of Electrical Power & Energy Systems, 2016; 83: 49-57.

[19] Castro CMBD, Marcato ALM, Souza RC, *et al*. The generation of synthetic inflows via bootstrap to increase the energy efficiency of long-term hydrothermal dispatches. Electric Power Systems Research, 2015; 124: 33-46.

[20] Khosravi A, Nahavandi S, Creighton D. A neural network-GARCH-based method for construction of prediction intervals. Electric Power Systems Research, 2013; 96: 185-193.

[21] Hyndman RJ, Fan S. Density Forecasting for Long-Term Peak Electricity Demand. IEEE Transactions on Power Systems, 2010; 25(2): 1142-1153.

[22] Wan C, Xu Z, Pinson P, *et al*. Probabilistic Forecasting of Wind Power Generation Using Extreme Learning Machine. IEEE Transactions on Power Systems, 2014; 29(3): 1033-1044.

[23] Arya R. Determination of customer perceived reliability indices for active distribution systems including omission of tolerable interruption durations employing bootstrapping. IET Generation, Transmission & Distribution, 2016; 10(15): 3795-3802.

[24] Othman MM, Musirin I. A novel approach to determine transmission reliability margin using parametric bootstrap technique. Electrical Power and Energy Systems, 2011; 33: 1666-1674.

[25] Xiao J, Gu W, Wang C, *et al*. Distribution system security region: definition, model and security assessment. IET Generation, Transmission & Distribution, 2012; 6(10): 1029-1035.

[26] Jiang T, Jia HJ, Jiang YL, *et al*. Cutset-angle based wide area thermal security region and its application in China southern power grid. International Transactions on Electrical Energy Systems, 2014; 24(11): 1600-1617.

[27] Yang TK, Yu YX. Static voltage security region-based coordinated voltage control in smart distribution grids. IEEE Transactions on Smart Grid, 2017; 9(6): 5494-5502.

[28] John F. Bootstrapping regression models. Available: http://citeseerx.ist.psu.edu/viewdoc/download?doi=10.1.1.182.9082&rep= rep1&type=pdf

[29] Orloff J, Bloom J. Bootstrap confidence intervals. Available: https://math.mit.edu/~dav/05.dir/class24-prep-a.pdf

[30] Thomas JD, Bradley E. Bootstrap confidence intervals. Statistical Science, 1996; 11(3): 189-228.